PAPER

Check for updates

An assessment of an ion exchange resin system for the removal and recovery of Ni, Hg, and Cr from wet flue gas desulphurization wastewater—a pilot study

Piotr Czupryński, [ID] *[ab] Maciej Płotka,[c] Piotr Glamowski,[b] Witold Żukowski [ID] [d] and Tomasz Bajda [ID] [a]

The paper presents the results of a pilot-scale study investigating the efficiency of an ion exchange resin system in the removal of Ni, Hg, and Cr from flue gas desulphurisation wastewater, in the presence of competitive metals such as Ca, Mg, Al, Fe, and Mn. The core part of the ion exchange installation consisted of two columns that were filled with ion exchange resin with iminodiacetic functional groups (Purolite S930) and one column filled with resin with isothiouronium functional groups (Purolite S920). The results showed that Ni, Hg, and Cr were almost completely removed from the wastewater with nearly 100% efficiency. Purolite S930 almost totally removed Ni, reducing its content from 89.3 ± 35 μg dm^{-3} to below 0.1 μg dm^{-3}, while Purolite S920 reduced the remaining Cr content from 2.2 ± 0.6 μg dm^{-3} and most of the Hg content, from 23.5 ± 6.6 μg dm^{-3} to below 0.1 μg dm^{-3}. The competitive metals Ca, Mg, Mn, and Al showed low affinity to the studied ion exchange resins. The study also assessed speciation of ion forms and sorption mechanisms. Breakthrough curve analysis was also carried out, which revealed that the selectivity sequence of iminodiacetic resin was Ni > Cr > Hg > Fe > Al > Mn > Ca, Mg. Elution studies were performed on S930 resins that allowed the separation of two streams: one containing mostly Ni and Fe which can be subjected to Ni recovery and the other containing mostly Cr and Hg which can be separated.

1. Introduction

According to global reports on the future of the power sector, the transition from fossil fuels to renewables is currently underway, although coal will continue to remain as a significant component of the global fuel mix until 2050.[1] As a result, pollution prevention related to coal combustion will be prioritized during the operation of these fuel-fired power plants. Sulphur is one of the important pollutants originating from coal and is emitted in the form of sulphur oxides. During the last few years, the EU has implemented an investment program to reduce pollutant emissions. One of the most technically and economically effective technologies applied was wet flue gas desulphurisation (wetFGD) which uses lime (calcium carbonate) as a reagent. This process allows the reduction of sulphur emission with an efficiency of above 90%.[2] In 2017, the

European Commission issued a new regulation governing emissions from the fossil fuel-generating power sectors. The document lists the new best available techniques (BAT) for large combustion plants, under Directive 2010/75/EU of the European Parliament and of the Council.[3] The regulation also has a new requirement for wastewater generated by wetFGD systems (flue gas desulphurisation wastewater—FGDW). Among the pollutants to be controlled in wastewater are metals and metalloids, such as Hg, Cd, Ni, As, Cr, Cu, Zn, and Pb. Table 1 presents the

[a] AGH University of Science and Technology, Faculty of Geology, Geophysics and Environmental Protection, Al. Mickiewicza 30, 30-059 Kraków, Poland. E-mail: piotrczuprynski@agh.edu.pl

[b] PGE Energia Ciepła S.A., ul. Złota 59, 00-120 Warszawa, Poland

[c] Purolite sp. z.o.o., 81-969 Gdynia, Poland

[d] Cracow University of Technology, Faculty of Chemical Engineering and Technology, Warszawska 24, 31-155 Kraków, Poland

Table 1 BAT-AELs for direct discharges to a receiving water body from flue-gas treatment

Element	BAT-AELs daily average [μg dm^{-3}]
As	10–50
Cd	2–5
Cr	10–50
Cu	10–50
Hg	0.2–3
Ni	10–50
Pb	10–20
Zn	50–200

RSC Advances

BAT-AELs (Best Available Techniques—Associated Emissions Levels) of metals and metalloids for direct discharges to a water body from flue gas treatment. FGDW is a type of industrial effluent. Its chemical composition strongly depends on the type of coal-fired, flue gas treatment methods used before the wetFGD process, including the type of equipment used for dust removal (*i.e.* electrostatic precipitator) or NOx removal (catalytic or noncatalytic). Besides sulphur, the wetFGD process also effectively eliminates volatile pollutants, such as F, As, B, Cl, Se, or Hg, in a gaseous form and/or as particulate matter (*i.e.* Pb, Cd, Zn, Cu, As, Cr). Once captured, a certain proportion of the trace pollutants is partitioned into solid by-products (gypsum) and water streams, including the wastewater discharged from the FGD system.[4] The FGDW can be characterized as a gypsum-saturated water solution containing trace elements that have partitioned into the absorber slurry.[5] This slurry is recycled through the FGD system until the concentration of chloride reaches a level that can pose a corrosion risk to the FGD unit. In general, chloride concentration is maintained at <20 000 mg dm^{-3} by diverting a slip stream for treatment through corrosion-resistant scrubber materials that allow some systems to maintain chloride concentrations as high as 40 000 mg per day.[6]

Recirculation leads to noticeable enrichment of some trace inorganic pollutants in water streams. However, it could also result in technical problems such as fouling of the absorber and pipes of the FGD system as well as environmental problems due to exceeding discharge limits for wastewater or gypsum.[7] Therefore, it is necessary to remove concentrated inorganic compounds continuously or periodically from the absorber. It is mainly realized by gypsum processing using a system of hydro cyclones, presses, or centrifuges. During this process, a part of the filtered water is recycled into absorber and a controlled amount is directed to the wastewater treatment plant.[8]

Table 2 presents the chemical composition and typical characteristics of FGDW.[9]

Different methods have been proposed for the removal of pollutants from FGDW. Pollutant removal from wastewater, is primarily achieved using an appropriate combination of physical, chemical, and biochemical processes, based on the pollutant to be removed. The commonly used combinations of methods are coagulation–flocculation–precipitation and sedimentation–filtration–flotation.[9–13] In these methods, suspended solids formed by remaining gypsum and fly ash are removed at the first step, and in the next steps chemical agents such as inorganic and organic sulphides are used to precipitate metals. A disadvantage of these methods is the production of sludge which is considered as a hazardous waste due to its high concentration of heavy metals.

One of the techniques applied for the removal of metals and metalloids is ion exchange with the use of specially designed resins. Due to their unique properties, such as fast kinetics, high treatment capacity, high removal efficiency, and cation selectivity, ion exchange resins have been widely used to remove heavy metals and metalloids from different types of wastewaters.[14] Ion exchange resin, either natural or synthetic, has the ability to selectively exchange its cations (H^+, Na^+) with the

Table 2 Typical characteristics of FGDW[9]

Parameter	Value
Temperature, °C	30–60
pH	4–9.5
Suspended solids, mg dm^{-3}	<40–10 000
COD, mg dm^{-3}	15–150
Cl^-, mg dm^{-3}	6000–40 000
SO_4^{2-}, mg dm^{-3}	1000–8000
S^{2-}, mg dm^{-3}	<0.2
SO_3^{2-}, mg dm^{-3}	<20
NO_3^+, mg dm^{-3}	50–1500
F^-, mg dm^{-3}	30–200
Ca, mg dm^{-3}	4000–22 000
Mg, mg dm^{-3}	200–5600
Na, mg dm^{-3}	75–1200
NH_4^+ mg dm^{-3}	<10–100
As, mg dm^{-3}	0.05–3
Al, mg dm^{-3}	50–800
B, mg dm^{-3}	20–40
Cd, mg dm^{-3}	0.04–0.5
Cr, mg dm^{-3}	0.3–5
Co, mg dm^{-3}	0.05–0.5
Cu, mg dm^{-3}	0.1–1
Fe, mg dm^{-3}	30–400
Pb, mg dm^{-3}	0.1–3
Hg, mg dm^{-3}	0.05–0.8
Ni, mg dm^{-3}	0.2–6
Se, mg dm^{-3}	0.2–1
V, mg dm^{-3}	0–2.4
Zn, mg dm^{-3}	0.4–10

metals' cations in the wastewater. Synthetic resins are widely preferred for ion exchange processes as they are highly stable and can effectively remove heavy metals from solution.[15]

The ion exchange reaction can be either reversible or irreversible. In the case of reversible reaction, the ion exchanger can be reused many times, even after regeneration.

Ion exchange resins consist of a crosslinked polymer matrix to which charged functional groups are attached by covalent bonds. The type of functional group plays an important role in the selective removal of metal cations from solution.[16] Ion exchange process involves the following steps: loading of resins during the treatment of solution, backwash with water, elution, regeneration, and rinse. Once the ion exchange sites on the resin are completely full, the resin must be regenerated for reuse.

Sodium hydroxide solution or mineral acid is mostly used in the regeneration.[17]

Some studies have used ion exchange resins for the removal of metal ions from water or wastewater. For example, a study applied ion exchange resins for the removal of hexavalent chromium from wastewater originating from the leather industry.[18] Another study used ion exchange resins for the purification of acidic waste streams containing heavy metals such as Cu(II), Zn(II), and Ni(II) in low and adjusted pH ranges as well as high concentration of NaCl.[19] Ion exchange is also frequently used to recover economically valuable ions from different effluents. For industry, rhenium was recovered from leaching solution released from copper industry.[20] Knowledge

regarding the effectiveness of ion exchange resins in the removal of multiple cations from FGDW is limited. A study assessed the effectiveness of ion exchange technique for selenium removal,[19] and attempts have been made to remove Hg, B, and Se by using ion exchange resin and other types of sorbents.[21] A pilot study focused on mercury removal using combined ultrafiltration–ion exchange method.[22] Most of the available studies have assessed basic parameters such as kinetics and were carried out in the laboratory scale.[23–25] It is clear from the literature that although ion exchange resins have been studied for the removal of metals and metalloids from different types of wastewaters, their applications in the treatment of FGDW are rather limited.

This paper presents the results of a pilot-scale study that analyzed the effectiveness of ion exchange resin system in the removal of hazardous metals and metalloids such as Ni, Hg, and Cr. The study tested an innovative approach based on the application of a system of ion exchange resins for the removal of a group of ions from real FGDW effluent. A pilot-scale system with a flow capacity of 1.2 m^3 h^{-1} and resin volume of 200 dm^3 was used for understanding the behavior of ion exchangers in conditions that are almost close to full-scale installations. The objective of this study was to assess the efficiency of the system of ion exchange resins in the removal of hazardous Ni, Hg, and Cr in the presence of co-occurring Al, Fe, Mn, Mg, and Ca cations as well as to analyze the possibility of separating and recovering Ni during elution.

2. Methods

2.1. Ion exchange resins

Two types of ion exchange resins were selected for the study: Purolite S930 (ref. 26) and Purolite S920.[27]

Purolite S930 is a macroporous polystyrene chelating resin containing functional iminodiacetic groups. It is used to capture heavy metal cations in wastewater containing a high concentration of monovalent cations, as well as to remove common multivalent cations (Ca, Mg, Fe, Al, Cu, Cd, Hg, Ni, Pb Zn, Co, Mo, Cr) from weakly acidic and weakly alkaline solutions. Purolite S930 is characterized by physical and chemical durability, and is thus suitable for extraction[28] and recovery of metals from ores,[29] plating solutions, pickling baths,[23,30] and wastewater, even in the presence of transition and precious metals. This resin is also useful for purifying a wide range of organic compounds[31] and inorganic materials from heavy metal contaminants mainly in aqueous solutions.[32] The bonds formed between metals and resins are sufficiently weak, and therefore, the resin bed can be easily regenerated at the end of the work cycle. Table 3 presents the properties of the S930 resin in detail.[26]

Purolite S920 is a macroporous polystyrene chelating resin containing isothiouronium functional groups for selective removal of mercury and is often used for recovering noble metals (Rh, Ru, Pt, Pd, Au, Ag) from a highly saline industrial solution and wastewater streams.[27,33] The speed of the exchange kinetics allows reducing mercury even at a low concentration, resulting in highly stable complexes with functional groups,

Table 3 Typical physical and chemical characteristics of S930 (ref. 26)

Polymer structure	Macroporous polystyrene crosslinked with divinylbenzene
Appearance	Spherical beads
Functional group	Iminodiacetic
Ionic form	Na$^+$ form
Copper capacity	50 g dm^{-3}
Moisture retention	52–60% (Na$^+$ form)
Particle size range	425–1000 μm
<425 μm (maximum)	2%
Specific gravity	1.18
Temperature limit	80 °C (176.0 °F)

with greater selectivity compared to other heavy metals.[34] Mercury and precious metals are strongly bound, and the expected time of one cycle is so long that regeneration of resin for reuse is uneconomical.[27] Table 4 presents the properties of the S930 resin in detail.

2.2. Pilot installation

The technological scheme of the pilot ion exchange installation is shown in Fig. 1. The installation received the sewage stream flowing from the FGDW treatment (FGD-WWTP) installation. Removal process in the FGD-WWTP suspension was carried out by coagulation and sedimentation. pH adjustment was done using calcium hydroxide. FeCl$_3$ was added as a coagulant after coagulation. Sludge was separated from the sewage in a lamella settling tank.

Before it reached the pilot installation, the wastewater stream was collected in a dedicated retention tank (RT) which was made of polypropylene and had a volume of 5 m^3. For technological reasons, this tank was equipped with a pH meter (Enderess + Hauser Orbisint CPS11D) and a turbidity meter (Enderess + Hauser Turbimax CUS52D) to measure the pH and turbidity of the wastewater, respectively. Then, the sewage was fed to the bag filter (BF) through a system of mutually reserve pumps (rotary lobe pumps, Börger AL-50), which had a maximum pump capacity of $Q = 3$ m^3 h^{-1}. Wastewater flow measurement unit (F) (Siemens Sitrans FM MAG5100 W) was installed downstream of the pumps. In the next stage, the wastewater reached the filtration node which removed residual solids remaining after sedimentation by BF (bag filter UNITEX,

Table 4 Typical physical and chemical characteristics of S920 (ref. 27)

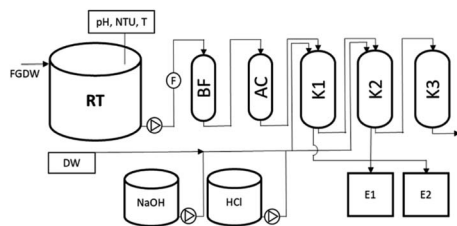| Polymer structure	Macroporous polystyrene crosslinked with divinylbenzene
Appearance	Spherical beads
Functional group	Isothiouronium
Ionic form	H$^+$ form
Mercury capacity	275 g dm^{-3}
Moisture retention	48–54% (H$^+$ form)
Particle size range	300–1200 μm
<300 μm (maximum)	1%
Specific gravity	1.11
Temperature limit	60 °C (140.0 °F)

Fig. 1 Technological scheme of the pilot installation used for testing ion exchange resins. FGDW—wastewater exiting the treatment plant; RT—retention tank; BF—bag filter column; AC—activated carbon column; K1, K2, K3—ion exchange resins; DW—demineralized water.

FWG 7, diameter 250 mm, height 920 mm, black carbon steel with anticorrosion coating) having a cartridge pore diameter of 20 μm, while the remaining organic compounds were removed by a column (UNITEX, FW-300, volume 170 dm³) filled with activated carbon (AC) (Sorbotech LG 95 bituminous activated carbon, grain size 0.6–2.4 mm, specific surface area 950 m² g⁻¹, volume 80 dm³). After mechanical and carbon filtration, the wastewater was directed to the ion exchange installation, where the ion exchange process was carried out in K1–K3 exchangers (UNITEX, WJ-500, volume 320 dm³) working in series.

The principle of operation of the ion exchange system was that the first two ion exchangers acted as the main purifying exchangers. Resins used in these exchangers were sorbents attached with cationic functional groups, which, under the process conditions, will bind cations with a valency of ≥2 (Ca, Mg, Fe, Al, Cu, Cd, Hg, Ni, Pb, Zn, Co, Mo, Cr).

The bonds formed between the sorbent and the cations were weak and nonselective enough to allow easy bed regeneration at the end of the work cycle. Columns K1 and K2 were filled with chelating ion exchange resin Purolite S930, at a volume of 200 dm³ each.

Columns K1 and K2 worked in series: Column 1 → Column 2. The system of pipelines and fittings ensured continuous operation of the installation—when one of the exchangers was switched on for elution/regeneration, the other exchanger remained in operation.

Column 3 was filled with Purolite S920 resin. This column was responsible for final polishing or removal of remaining mercury from the wastewater solution. The affinity of the resin for heavy metals is so strong that resin regeneration is not economically feasible. The bed, due to its high affinity, will be able to remove even the residual concentration of metals to the required level. After treatment in the pilot installation, the wastewater was directed back to the FGDW treatment plant.

Apart from the main line of operation, which includes the bag filter and K1–K3 columns, the pilot installation was equipped with an elution/regeneration system which included acid (HCl) and base (NaOH) feeding systems (equipped with dosing pumps) and 1 m³ tanks (E1–E2). The tanks collected the eluates and washing solutions after regeneration.

Among the three columns, only K1 and K2 containing regenerable resins were subjected to regeneration. Due to the high binding of metal cations for the resins in the K3 column, regeneration was not performed for this column.

2.3. Pilot installation run length and elution studies

The ion exchange working cycle consisted of two main stages: the first step involved loading of resins during wastewater treatment (service), and in the next step the resin column was set aside and elution and regeneration were performed. The appearance of Ni after K1 column was considered as the signal to begin the regeneration/elution stage.

During pilot installation, four cycles were carried out. In all cycles, the columns worked in series. The main objective of three first cycles was to optimize the parameters of the pilot installation: optimal flow rate, pH range, NTU value, concentrations, and chemical flow (HCl, NaOH, demineralized water). The paper presents the results of the optimized fourth cycle.

Removal efficiency (E, %) of selected metals was calculated for single ion exchange column as well as for the whole system. The formula used for calculation was as follows:

$$E = (C_0 - C_{eq.})/C_0 \times 100\%$$

where C_0 is the average concentration [mg dm⁻³ or μg dm⁻³] of Al, Ca, Mg, Fe, Mn, Ni, Hg, and Cr before passing through each column and $C_{eq.}$ is the concentration [mg dm⁻³ or μg dm⁻³] of metals after passing through all columns and the total system.

2.3.1. Breakthrough curve studies. To evaluate the performance of different resins during the loading stage of each column and to compare the behavior of different elements, a breakthrough curve analysis was carried out based on $C_{eq.}/C_0$ ratio *versus* BV (wastewater flow expressed as the volume of ion exchange resin bed). C_0 is the concentration [mg dm⁻³ or μg dm⁻³] of metals before passing through column and $C_{eq.}$ is the concentration [mg dm⁻³ or μg dm⁻³] of the metals after passing through each column. BV is the amount of treated wastewater, which was expressed as ion exchanger bed volume. The ratio values near 0 indicated that the resin removed the element with high efficiency, while values around 1 indicated that input and output concentrations were at the same level and the element was not bound by the resin or the resin was fully saturated by the given element. The analysis revealed the selectivity of analyzed metals for each column used and allowed predicting the moment of saturation for each element. Such analysis is often used in the assessment of performance and selectivity (in hydrometallurgy) of ion exchangers.[23] Table 5 presents the parameters of the installation during the analyzed cycle. The average flow of wastewater was 1.6 ± 0.2 m³ h⁻¹, the total amount of treated wastewater was 1127 m³ which corresponds to 5635 BV. Samples were captured during elution and HCl leaching by rinsing with demineralized water. Acid eluate and acid rinsing solution were collected separately in 1 m³ containers and analyzed.

Table 5 Parameters of work related to the analyzed cycle

	Unit	Value
Average flow	[m³ h⁻¹]	1.6 ± 0.2
Run length	[m³]	1127
Run length	[BV]	5635

2.3.2. Elution studies. The regeneration/elution started with backwash with water, followed by which 10% HCl was used for elution. In the last steps, rinsing was done with demineralized water, regeneration with 2% NaOH, and final rinsing with demineralized water. Regeneration/elution study was carried out only for columns K1 and K2. Eluates were sampled and collected after 1 BV of HCl was dosed, and dosing was stopped after 2 BV, followed by rinsing with demineralized water. The total volume of eluate collected for K1 after dosing 10% HCl was 120 L (0.6 BV), while 400 L (0.2 BV) of solution was collected during rinsing with demineralized water. In the case of K2, the volumes collected were 120 L (0.6 BV) and 530 L (2.7 BV), respectively.

2.3.3. Analysis of nonregenerable resin S920. After tests, ion exchange resin S920 in column K3 was washed and mixed with demineralized water.

A 10 dm^3 sample of the mixed resin was taken. Then, a representative 10 cm^3 sample was dried, mineralized, and analyzed by inductively coupled plasma-optical emission spectroscopy (ICP-OES).

2.4. Analytical methods and sampling

During the loading stage, a series of samples were collected after AC column and each ion exchange columns (K1, K2, and K3). The samples were filtered through a micromembrane filter of 0.45 μm to remove suspended particles. Before storage and transport to the laboratory, the pH of the samples was corrected by adding 0.5 ml of 20% HNO_3 aqueous solution. The samples were taken once every 48 hours. Samples were taken both after the specified dosing volumes of HCl and rinsing with demineralized water, and they were taken from the tanks in which the eluate and rinsing water were collected. ICP-OES was used to determine the concentrations of Ni, Hg, Cr, Al, Fe, Ca, Mg, and Mn in all the liquid samples. The samples were analyzed using an Optima 5300V PerkinElmer instrument which was calibrated using standards containing the elements to be analyzed.

2.5. Modeling of Ni, Cr, and Hg speciation

Speciation of Cr, Ni, and Hg in wastewater fed to ion exchange columns was modeled and assessed using Visual MINTEQ 3.1.[35] Modeling was carried out at a pH range of 6–7 with 0.1 steps.

3. Results and discussion

3.1. Chemical composition of FGDW

Table 6 presents the chemical composition of wastewater directed to ion exchange resins system, based on the data obtained for 10 samples taken after AC column and analyzed during the loading period which lasted 22 days.

The content of chlorides and sulphates was found to be in a lower range, which in FGDW can typically reach 40 and 8 g dm^{-3}, respectively.[9] The pH value that had an impact on the performance of ion exchange resins was 6.87 ± 0.29, and no significant variations in this parameter were observed. Due to the risk of resins bead fouling, it is important to maintain the level of suspended solids as low as possible. Throughout the

Table 6 Chemical composition of FGDW after filtration and activated carbon (AC) during pilot tests

Analyte	Unit	Average	SD
Data from pilot station monitoring			
Al	[μg dm^{-3}]	221.6	228.9
Ca	[mg dm^{-3}]	5575.6	981.9
Fe	[μg dm^{-3}]	66.5	110.2
Mg	[mg dm^{-3}]	224.2	32.8
Mn	[μg dm^{-3}]	155.6	236.8
Ni	[μg dm^{-3}]	89.3	35.0
Hg	[μg dm^{-3}]	36.9	32.4
Cr	[μg dm^{-3}]	59.3	20.7
pH		6.87	0.29
Data from existing FGD-WWTP monitoring			
Cl^-	[mg dm^{-3}]	8893.4	2491.5
SO_4^{2-}	[mg dm^{-3}]	860	62
Suspended solids	[mg dm^{-3}]	17.53	12.77

study, it was noted that before filtration and activated carbon treatment, the level of suspended solids was <30 mg dm^{-3}. Due to its origin, the wastewater fed to the columns was rich in Ca (above 5 g dm^{-3}) and Mg (ca. 200 mg dm^{-3}).

The coexisting cations of metals such as Fe, Al, and Mn did not exceed above 1 mg dm^{-3} and were at a similar level as the cations of hazardous metals (Ni, Hg, and Cr) analyzed in the study. Interestingly, a very high fluctuation of metal concentration was found, as was indicated by high standard deviation values which were very often higher than the average values. Table 6 presents the values for the period of 1 month. It can be seen that even during this short period, there were variations in the content of metals in the whole FGD system.

A key factor for fluctuations is the differences in trace element concentrations in the coal combusted by plant, where variations can be observed in the order of magnitude. Other sources of fluctuations can be operation and maintenance of flue gas cleaning installation, including the type of denitrification method used, where in the case of catalytic methods many metals can be oxidized to higher valence states.[36,37] Furthermore, the quality of lime used as an SO_x sorbent and water used for desulphurization of flue gases can have a significant impact on the final composition of FGDW.[7] Due to their nature, ion exchange resins are designed for specific removal of the ionic forms of selected metals. Thus, in the presence of forms like oxyanions, colloids, or suspended solids, the proposed ion exchange process will not effectively remove the other forms of Ni, Hg, and Cr. This was confirmed by the analysis of mercury removal, in which ion exchange resins did not show expected performance due to the presence of noncationic forms of metals in FGDW.[33,38]

To simulate the expected speciation of Ni, Cr, and Hg in the wastewater, modeling of speciation was carried out using Visual MINTEQ 3.1. The results of the modeling are presented in Fig. 2.

According to the modeling results, the dominant form of Ni in the solution was divalent cation Ni^{2+} which accounted for >90% of all species, while the other species were $NiSO_4(aq)$ and cations $NiCl^+$ and $NiOH^+$. The distribution of Ni forms was stable in the analyzed pH range. Similarly, in the studied pH
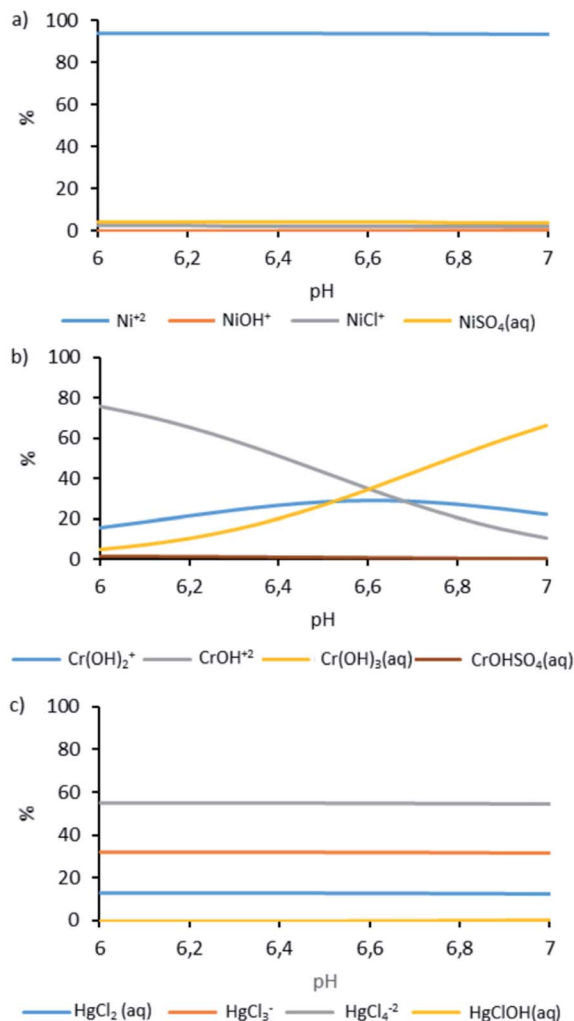
Table 7 Removal efficiency [%] of separate ion exchange columns and total system

Element	K1	K2	K3	Total system
Al	−25.0%	30.4%	−14.4%	0.4%
Ca	1.4%	1.3%	−0.2%	2.4%
Fe	80.3%	75.7%	−264.6%	82.6%
Mg	0.3%	1.6%	0.8%	2.7%
Mn	19.9%	75.3%	−415.1%	−2.0%
Ni	95.9%	100.0%	—	100.0%
Hg	7.0%	17.9%	100.0%	100.0%
Cr	89.9%	66.7%	100.0%	100.0%

significantly bound this element, while at the next steps after columns K2 and K3 no removal of Fe ions was observed and after K3 the average concentration was found to be increased.
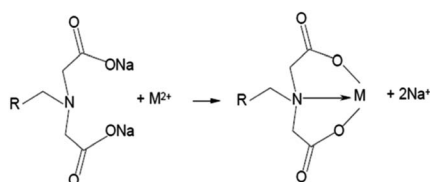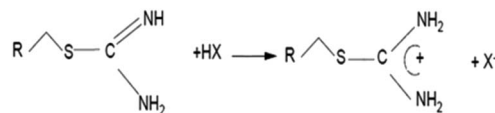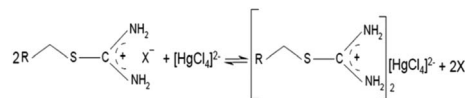
Table 7 summarizes the observed removal efficiency for each column and for the total system used.

As mentioned in the section, the hazardous elements Ni, Hg, and Cr were removed 100% to values below the detection limit (<0.1 μg dm^{-3}). Among co-occurring ions, Fe was removed effectively, while the removal of Al and alkaline earth metals Ca and Mg was negligible. Low and especially negative removal efficiencies observed for these elements indicate the fact that the metals that were already bound to the resin were replaced by those with higher affinity. This was true in the case of Fe and Mn for which high negative removal efficiency was observed in column K3.

For columns K1 and K2, the presence of two carboxyl groups and tertiary nitrogen atom in the iminodiacetic functional group resulted in strong affinity for Cr(III) and Cu(II).[39] In neutral and alkaline systems, the group forms complexes through the reaction presented in Scheme 1.[16]

The presented mechanism clearly explains the removal of Ni as well as the high affinity of columns K1 and K3. Ni was mostly present as an Ni^{2+} cation in the studied wastewater as revealed by the simulation analysis performed using Visual MINTEQ 3.1. software. Cr speciation showed that the cationic forms of chromium hydroxides of the element were dominant (Cr(OH)$_2$$^+$ and CrOH^{2+}) at pH near 6 while nondissociated Cr(OH)$_3$(aq) was dominant at pH around 7. The observed removal efficiency suggested that S930 still had significant affinity to the cationic forms of chromium hydroxides. Modeling of Hg speciation revealed that the dominant forms in the treated solution were HgCl$_4$$^{2-}$ and HgCl$_3$$^-$ anions.

According to the mechanism proposed by Z. Hubicki and D. Kołodyńska,[16] depending on the pH, the isothiouronium groups present in column K3 occurred in the forms presented in Scheme 2.

Scheme 1 Reaction of iminodiacetic group and metal cation.

Scheme 2 Forms of isothiouronium group depending on pH.

Scheme 3 Anion exchange mechanism of isothiouronium group.

The first form in low pH formed coordination bond, whereas for the second form in high pH the sorption process proceeded in accordance with the anion exchange mechanism presented in Scheme 3.

The mechanism shown in the scheme explains the high efficiency of removal of anionic Hg forms present in the solution.

As mentioned in earlier studies,[22,38] the analyzed elements can also exist in the form of microsuspension and colloidal particles, especially precipitated Hg and Cr. Therefore, in this situation, removal is only possible through filtration by microporous structure of the resins. This can be seen in S920, for which it is difficult to explain the achieved level of removal of Hg and Cr by ion exchange with iminodiacetic functional groups.

Taking into account the BAT-AELs, according to which the thresholds for Ni, Hg, and Cr are 10–50, 0.2–3, and 10–50 μg dm^{-3}, and the final concentrations of the analyzed heavy metals were below the detection limit of <0.1 μg dm^{-3}, the proposed ion exchange resin system could be potentially used for FGDW treatment.

3.3. Breakthrough curve studies

The operation of the used system of ion exchange columns was characterized by performing the C/C_0 breakthrough analysis. To better illustrate the behavior of each metal, the figures corresponding to each column (K1, K2, K3) are divided and presented as two graphs, with the first one (a) dedicated to alkaline earth metals Ca and Mg and co-concurring metals Al and Fe and the second one (b) to Ni, Hg, and Cr. The breakthrough curves for column K1 are presented in Fig. 5.

It can be observed that Ca and Mg almost had no affinity to the iminodiacetic functional groups used in the S930 resin. The C/C_0 ratio for these metals was close to 1 throughout the study. By contrast, Mn appeared in the effluent from K1 after around 500 BV and Al after 750 BV, with a C/C_0 ratio of >2, which means that the concentrations of these elements were twice or higher in the effluent of the column than in the influent. This proves that Al and Mn were bound by K1; however, the bonds were quite weak and the ions of these elements were quickly replaced by those having higher affinity to iminodiacetic groups. The behavior of Fe ions showed that the ions were removed, and variation was observed in the removal of this element between 1000 and 2000 BV, with the C/C_0 ratio reaching 0.5.
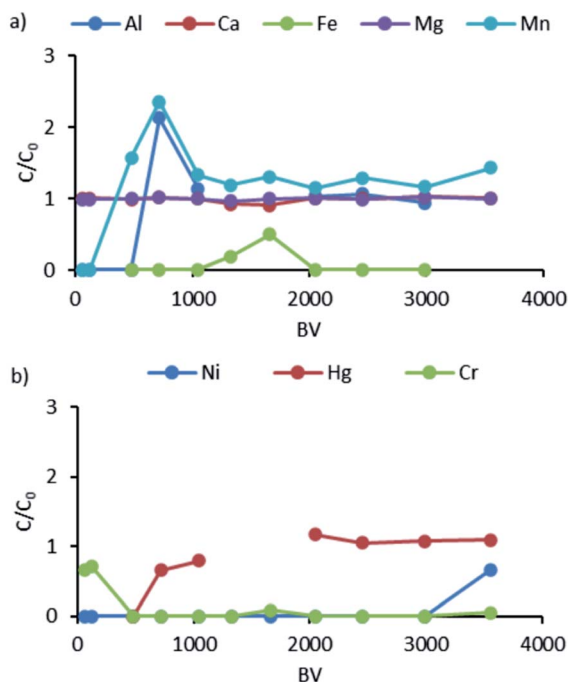
Fig. 5 Breakthrough curves for K1: (a) data for Al, Ca, Fe, Mg, and Mn; (b) data for Ni, Hg, and Cr.

This is due to the fact that, as in the case of Mn and Al, iron, after binding to the ion exchange resin, was displaced by other ions that can form stronger bonds. Ni was successfully removed from the wastewater almost during the whole loading phase, and only at the end of the period the breakthrough appeared on the column (after 3500 BV), which was a signal to begin the elution/regeneration phase. Cr ions were also successfully bound by the resin, at the beginning of the loading phase, with a C/C_0 ratio of around 0.7. However, a different trend was observed for mercury. As in the case of Al and Mn, the forms of mercury present in the wastewater ($HgCl_4^{2-}$, $HgCl_3^{-}$, $HgCl_2$) broke through quite quickly (*ca.* 750 BV). The gap observed in the plot between 1300 and 1700 BV for Hg was due to the mercury concentration before K1, which was below the limit of detection (<0.1 µg dm^{-3}).

The next factor that can impact the binding of ions to a corresponding ion exchanger is the presence of other competing ions, especially if their concentrations are significantly higher by several orders of magnitude. The influence of competitive ions could be expected, especially in the case of Ca, Mg which concentrations are at the level of 5 g dm^{-3} in the case of Ca and 500 mg dm^{-3} for Mg. The concentrations of these ions are over 1000 times higher than the analyzed Ni, Cr and Hg. The obtained results indicate that even such a high difference in concentration did not significantly affect Ni binding by the S930 resin. The effect of a much higher concentration of competing cations may impact the binding kinetics or possibly cause a reduction in the sorption capacity of the resin. In the case of Cr and Hg, the ionic form, *i.e.* the anionic form in the case of mercury or the nondissociated form in the case of Cr (according to the modelling results presented in Fig. 2), may play a much

more significant role in the binding than the presence of Ca and Mg in *ca.* 1000 times higher concentrations.

In the K2 column containing the same ion exchange resin, similar behavior of the analyzed elements was observed as in K1 (Fig. 6). This means that Ca and Mg were not removed at all (C/C_0 ratio around 1), while Al and Mn were bound and released quite quickly (C/C_0 ratio above 1.5). After K1, the remaining Ni was completely removed from the solution. The C/C_0 ratios for Ca and Mg were almost 1, which indicates the low affinity of ions of the elements for the resin. Based on the analysis of Al and Mn, the time shift in the breakthrough of these ions through the exchangers compared to K1 was marked. The difference was approximately 200–300 BV.

For iron, a high C/C_0 value of 2.5 was recorded, which may indicate that this ion was displaced by others or that the deposited ion was rapidly released as a microsuspension or other that has no affinity to the resin. K2 removed the remaining Ni after K1 to the lowest possible concentration that can be detected by the analytical method used. Hg appeared at the exit from K2 after 2000 BV, and C/C_0 values around 1 suggested that the ion exchange process did not remove this element. It should be noted that the ion exchange process takes place gradually: first the H^+ ions are exchanged for Na^+ and then the functional groups bind the appropriate heavy metal cations.[40] This causes changes in the pH of the solution, which can lead to precipitation or co-precipitation of individual metal cations.[32]

Based on the breakthrough behavior of various metals observed in this study, it can be assumed that their removal by iminodiacetic resins follows a selectivity sequence for the analyzed wastewater as shown below:
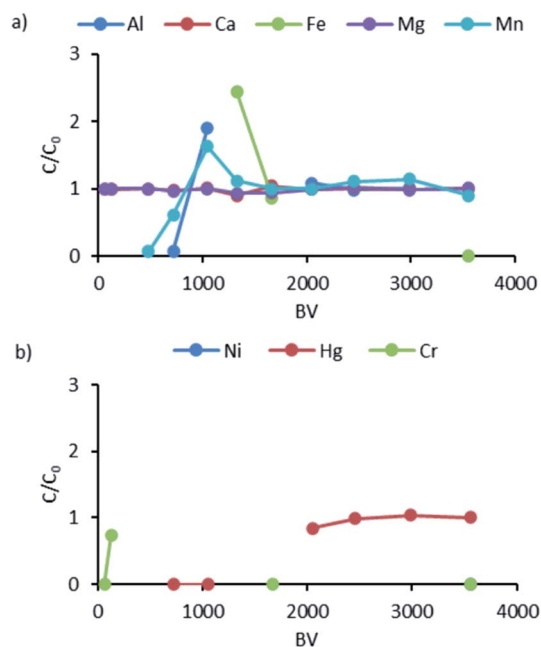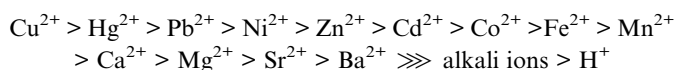
$$Ni > Cr > Fe > Al > Mn > Ca, Mg$$

Fig. 6 Breakthrough curves for K2: (a) data for Al, Ca, Fe, Mg, and Mn; (b) data for Ni, Hg, and Cr.

According to the literature,[16] the selectivity sequence for iminodiacetic chelating resins is as follows:

$$Cu^{2+} > Hg^{2+} > Pb^{2+} > Ni^{2+} > Zn^{2+} > Cd^{2+} > Co^{2+} > Fe^{2+} > Mn^{2+}$$
$$> Ca^{2+} > Mg^{2+} > Sr^{2+} > Ba^{2+} \ggg \text{alkali ions} > H^+$$

Comparing the data obtained from the study and the data in the literature, a difference was noted in the order of Ni and Hg. This may indicate the presence of mercury in various forms, of which the Hg^{2+} ionic form is not dominant in the studied wastewater. Based on the speciation diagram presented by P. J. Lloyd-Jones et al.,[34] in water solution with a high concentration of chlorides at a pH between 6 and 7, Hg can be present in different forms such as $HgCl_2$, $HgCl^+$, $HgCl_3^-$, $Hg(OH)_2$, $HgOH^+$, Hg_2^+, and $HgCl_4^{2-}$. Of these, the dominant form is uncharged $HgCl_2$, which, in the pH range of 6–7, is successively replaced by the uncharged $Hg(OH)_2$ form, while the other forms can only exist in traces. The breakthrough curve analysis for K3 is presented in Fig. 7.

As illustrated, Al, Ca, Fe, Mg, and Mn were not removed at all in K3 (Fig. 7). Based on the plots, the C/C_0 ratios were determined to be 0, which means that the resin bound all Hg and traces of Cr. It should be noted that higher C/C_0 values indicate the fact that the ions already sorbed (especially Mn, Fe) to the resin metals are replaced by those with a higher more affinity.

The results suggest that isothiouronium functional group applied in the resin can also remove ions other than Hg^{2+}. However, the binding of Hg by S920 seems to be much more complex and involves the formation of a coordination bond between Hg and sulphur and amine in the functional group.[34] A simplified mechanism of removal of Hg by the anion exchange process has been described in the literature.[16] The details of the reaction are unknown, but the reaction may probably resemble the binding mechanisms found in protein systems.[41] Additionally, as shown in Scheme 3, the anionic forms of mercury that are found in the studied pH range, $HgCl_4^{2-}$ and $HgCl^{3-}$, can be bound via the anion exchange mechanism proposed by Z. Hubicki and D. Kołodyńska.[16]

3.4. Elution studies

After the K1 and K2 column loading phase, an elution step was performed, at which 10% HCl was used for eluting the bound cations from ion exchange resins and demineralized water was used to flush the acid and remaining anions. HCl dosing was stopped at 2 BV, followed by rinsing with demineralized water to 4 BV. The concentrations of metals achieved versus the volume of the reagent used (elution profiles) are presented in Fig. 8.

The first remarkable difference noted between the metal profiles is the order of magnitude of the concentrations measured for individual elements. Ca, Mg, Fe, and Ni were measured in mg dm^{-3}, while Al, Mn, Hg, and Cr were measured in µg dm^{-3}.

After 10% HCl was drawn into the column, as reflected by a sharp increase in the concentration of Ca, Mg, Ni, Fe, and Mn on the resin, the ions were displaced by highly concentrated H^+
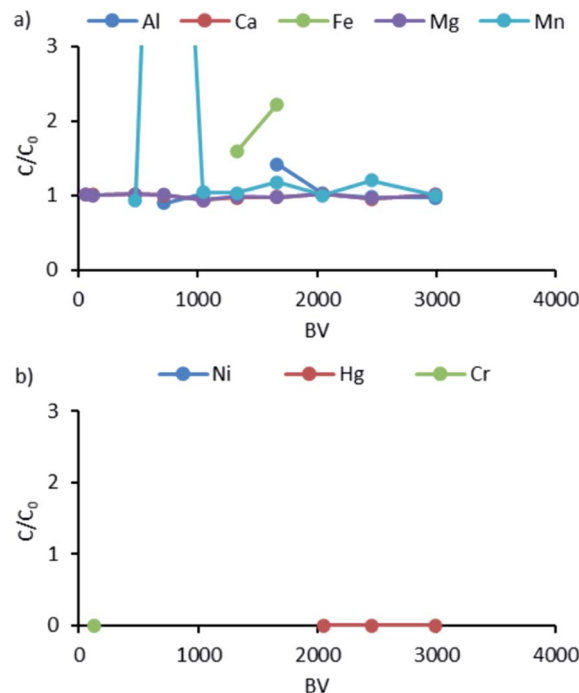

Fig. 7 Breakthrough curves for K3: (a) data for Al, Ca, Fe, Mg, and Mn; (b) data for Ni, Hg, and Cr.

ions and eluted with spent HCl. The peak of the metal ions was observed at about the same time between 1.2 and 1.5 BV.

The peak concentrations of Ca, Mg, and Fe were remarkably high and exceeded 4500, 1500, and 1100 mg dm^{-3}, respectively. Among the metal ions studied, i.e., Ni, Hg, and Cr, the highest concentration was recorded for Ni, with a peak concentration of 419 mg dm^{-3}. The highest recorded concentrations for Cr and Hg were 400 and 100 µg dm^{-3}, respectively. It is worth mentioning that Cr and Hg peaks occurred only in the resin

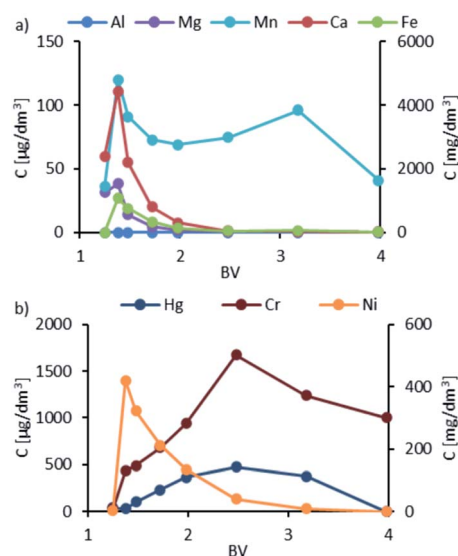Fig. 8 Elution profiles of K1: (a) data for Al and Mn in µg dm^{-3}, and Mn, Ca, and Fe in mg dm^{-3}; (b) data for Hg and Cr in µg dm^{-3} and Ni in mg dm^{-3}.

Fig. 9 Elution profiles of K2: (a) data for Al and Mn in $\mu g \, dm^{-3}$, and Mn, Ca, and Fe in $mg \, dm^{-3}$; (b) data for Hg and Cr in $\mu g \, dm^{-3}$ and Ni in $mg \, dm^{-3}$.
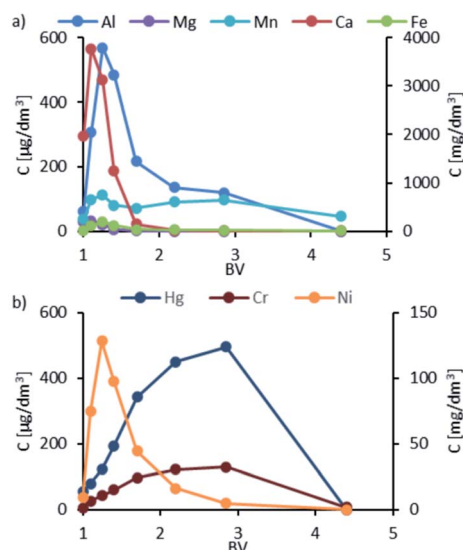
washing phase at BV values. For Mn ions, two peaks were noted: the first one when dosing HCl where the concentration of the ions was 120 $\mu g \, dm^{-3}$ and the second one when rinsing with demineralized water at around 3–35 BV, with the concentration reaching 100 $\mu g \, dm^{-3}$. Al ions were not detected in the elution and rinsing phase. The elution profiles for K2 are presented in Fig. 9, which are similar to the K1 column. A key exception is the appearance of Al with the peak occurring at the HCl dosing stage, with the highest concentration of 569 $\mu g \, dm^{-3}$. In general, the concentrations of metals in eluates were lower compared to that in K1.

This was expected because K2 acted as a protective column against the breakthrough of metal ions, mainly Ni and Cr. The absence of Al ions in the eluate and washing solution in K1, as well as the presence of Al ions in K2, may indicate that these ions are weakly bound by iminodiacetic groups and are quickly replaced by the ions of other metals.

The possibility of recovering metals was assessed by analyzing the eluates and rinsing solutions from K1 and K2. A 120 dm^3 sample of eluates was collected from K1 and K2, and 400- and 530 dm^3 samples of rinsing solution were collected

from K1 and K2, respectively. Table 8 presents the concentrations of metals in this solution in comparison to feed FGDW.

The concentrations of Ni and Fe in eluates were about 1000–2000 times higher than in the feed wastewater, while the concentrations of Hg and Cr were about 10 times higher. In the case of Ca and Mg, no such increase in concentration was observed. These results confirm that columns K1 and K2 can selectively remove mostly Ni and Fe.

The data obtained from the elution studies showed that it is possible to separate small volumes of a solution stream containing the most concentrated metals such as Ni and Fe and to direct the stream to processes that allow the recovery of Ni. This suggests that resins with iminodiacetic groups have a low affinity to Ca, Mg, and Mn. Cr and Hg can be separated from the stream of residual metals by rinsing with demineralized water.

However, the recorded concentrations were at a low level of several hundred $\mu g \, dm^{-3}$. Therefore, it is recommended that these solutions should be recycled to the wastewater treatment process, where mercury will already be removed by the resin with isothiouronium functional groups.

Two different peaks of metals were observed in the elution study: the first when HCl was used and the second when demineralized water was used to remove the acid from the column. The first peak can be attributed to ion exchange between bound cations and H^+ provided by the strong acid HCl.

There is a change in the equilibrium of the metal cation binding reaction during the regeneration process. The change is due to using of an acid solution with a relatively high concentration of 10% HCl and thus the concentration of H^+ cations. In line with Le Chatelier's principle, the balance of the reaction will be shifted towards the binding of H^+ ions and the release of cations of other previously bound metals.

On the other hand, the second peak is much more difficult to explain. One of the important factors determining the effectiveness of ion exchange is convective/dispersive transport in porous medium between particles and diffusive transport within the boundary layer around the particles (Nernst film). The diffusive transport in boundary layer is significantly slower than convective/dispersive transport between particles and can significantly influence the ion exchange kinetics.[11] During washing with demineralized water and HCl displacement in the resin, higher concentrations of Cl^-, and in general dissolved ions, found in the Nernst film compared to the external solution

Table 8 Concentration of metals in eluates and rinsing solution in comparison to feed wastewater

Element	Unit	K1		K2		Average in feed FGDW
		Eluate	Rinsing solution	Eluate	Rinsing solution	
Al	[$\mu g \, dm^{-3}$]	0	0	800	123	222
Ca	[$mg \, dm^{-3}$]	1341	34	1884	49	5576
Fe	[$mg \, dm^{-3}$]	442	25	116	14	0.066
Mg	[$mg \, dm^{-3}$]	8	1	9	1	224
Mn	[$\mu g \, dm^{-3}$]	92	63	86	67	156
Ni	[$mg \, dm^{-3}$]	246	19	94	5	0.089
Hg	[$\mu g \, dm^{-3}$]	222	194	162	167	37
Cr	[$\mu g \, dm^{-3}$]	673	706	64	43	59

Table 9 Concentrations of metals bound by S920

Element	Unit	Value
Hg	$[mg\ kg^{-1}]$	7510
Cr	$[mg\ kg^{-1}]$	38.7
Ni	$[mg\ kg^{-1}]$	21.6

could be a driving force for leaching of retained metals. A very high ΔC results in the elution of sorbed chloride and hydroxy ions of Cr and Hg.

3.5. Analysis of nonregenerable resin S920

Additionally, to identify the ions sorbed on the S920 resin, an analysis was carried out on the elements bound by the material. The concentrations of metals sorbed on the nonregenerable resin are presented in Table 9.

It was observed that the S920 resin mostly accumulated Hg, the concentration of which was 7510 mg kg^{-1} of the resin. This confirms the high affinity of the resin to the Hg compounds in FGDW. In case of Cr and Ni the concentrations of the element on the resin were 38.7 and 21.6 mg kg^{-1} respectively. This may prove that this resin removed the residual amounts of Cr and Ni remaining after columns K1 and K2.

4. Conclusions

Based on the results of the study, the following conclusions could be drawn:

• The tested ion exchange system consisting of iminodiacetic and isothiouronium functional groups was ideal for selective removal of Ni, Hg, and Cr from FGDW.

• The ion exchange process was effective in the presence of competing metals such as Ca, Mg, Al, Fe, and Mn.

• The modeled Ni speciation showed that Ni^{2+} is the main form of the element that explains the obtained results. Ni^{2+} is mostly removed in the ion exchange process where the cation creates complexes with iminodiacetic functional groups.

• The lower affinity of Cr to iminodiacetic group was related to its form in the wastewater ($CrOH_2^+$, $Cr_2(OH)_2^{4+}$, and $Cr(OH)_3(aq)$).

• The modeled forms of Hg were $HgCl_4^{2-}$, $HgCl_3^{-}$, $HgCl_2$, and HgClOH, and in the case of isothiouronium group in nonacidic pH the sorption process proceeded according to the proposed anion exchange mechanism.

• The elements Ca, Mg, Mn, and Al showed low affinity to selected ion exchange resins, which suggests that they can be easily replaced by other cations.

• The breakthrough behavior analysis of the studied metals indicated that the removal of these metals by iminodiacetic resins followed a selectivity sequence: Ni > Cr > Hg > Fe > Al > Mn > Ca, Mg.

• The tested elution sequence revealed that the proposed process allowed separating two effluent streams: the first containing most of Ni and Fe, which can then be subjected to various hydrometallurgical processes for recovering Ni, and the second containing most of Cr and Hg, which can be separated during elution.

Conflicts of interest

There are no conflicts to declare.

Acknowledgements

References

1 International Energy Agency, *World Energy Outlook 2020*, 2020.

2 P. Córdoba, Status of Flue Gas Desulphurisation (FGD) systems from coal-fired power plants: Overview of the physic-chemical control processes of wet limestone FGDs, *Fuel*, 2015, **144**, 274–286.

3 European Commission, *Commission Implementing Decision (EU) 2017/1442 of 31 July 2017 establishing best available techniques (BAT) conclusions, under Directive 2010/75/EU of the European Parliament and of the Council, for large combustion plants*, 2017.

4 P. Córdoba, R. Ochoa-Gonzalez, O. Font, M. Izquierdo, X. Querol, C. Leiva, M. A. López-Antón, M. Díaz-Somoano, M. R. Martinez-Tarazona, C. Fernandez and A. Tomás, Partitioning of trace inorganic elements in a coal-fired power plant equipped with a wet Flue Gas Desulphurisation system, *Fuel*, 2012, **92**(1), 145–157.

5 C.-M. Cheng, P. Hack, P. Chu, Y.-N. Chang, T.-Y. Lin, C.-S. Ko, P.-H. Chiang, C.-C. He, Y.-M. Lai and W.-P. Pan, Partitioning of Mercury, Arsenic, Selenium, Boron, and Chloride in a Full-Scale Coal Combustion Process Equipped with Selective Catalytic Reduction, Electrostatic Precipitation, and Flue Gas Desulfurization Systems, *Energy Fuels*, 2009, **23**, 4805–4816.

6 Electric Power Research Institute, Conditions Impacting Treatment of Wet Flue Gas Desulfurization Wastewater, Palo Alto, CA, Electric Power Research Institute, 2007.

7 P. Córdoba, O. Font, M. Izquierdo, X. Querol, A. Tobías, M. A. López-Antón, et al., Enrichment of inorganic trace pollutants in re-circulated water streams from a wet limestone flue gas desulphurisation system in two coal power plants, *Fuel Process. Technol.*, 2011, **92**, 1764.

8 United States Environmental Protection Agency, Final Effluent Limitations Guidelines and Standards for the Steam Electric Power Generating Industry, 2015.

9 A. M. Carpenter, *Wastewater regulations and issues for coal-fired power plants*, IEA Clean Coal Centre, CCC/283, February 2018.

10 European Commission, Best Available Techniques (BAT) Reference Document for Large Combustion Plants, Industrial Emissions Directive 2010/75/EU, Integrated Pollution Prevention and control, 2017.

11 A. Mabrouk, V. Lagneau, C. De Dieuleveult, M. Bachet, H. Schneider, et al., Experiments and modeling of ion exchange resins for nuclear power plants. International Journal of Engineering and applied sciences, *Int. J. Eng. Appl. Sci.*, 2012, **6**, 130–134.

12 Eurelectric, *Eurelectric proposal for LCP BREF 2006*, 2001.

13 Siemens, *Filtrat. Separ.*, 2009, **46**(4), 8.

14 S. Y. Kang, J. U. Lee, S. H. Moon and K. W. Kim, Competitive adsorption characteristics of Co2+, Ni2+, and Cr3+ by IRN-77 cation exchange resin in synthesized wastewater, *Chemosphere*, 2004, **56**, 141–147.

15 B. Alyüz and S. Veli, Kinetics and equilibrium studies for the removal of nickel and zinc from aqueous solutions by ion exchange resins, *J. Hazard. Mater.*, 2009, **167**, 482–488.

16 Z. Hubicki and D. Kołodyńska, *Ion Exchange Technologies Chapter 8: Selective Removal of Heavy Metal Ions from Waters and Waste Waters Using Ion Exchange Methods*. IntechOpen, 2012.

17 EPA, *Reference Guide to Treatment Technologies for Mining-Influenced Water*, 2014, EPA 542-R-14-001.

18 N. O. Isik and M. (Koizhaiganova) Kaygusuz, Removal of chromium(vi) from aqueous solutions by anion exchange resins, *Oxid. Commun.*, 2017, **40**(4), 1384–1391.

19 T. Nishimura, R. Hata and Y. Umetsu, *Minor elements 2000: processing and environmental aspects of As, Sb, Se, Te, and Bi*, 2000, pp. 355–362.

20 Z. Bo, L. Hong-Zhao, W. Wei, G. Zhao-Guo and C. Yao-Hua, Recovery of rhenium from copper leach solutions using ion exchange with weak base resins, *Hydrometallurgy*, 2017, **173**, 50–56.

21 A. Ohki, K. Yamada, T. Furuzono, T. Nakajima and H. Takanashi, Analysis of Trace Elements in Flue Gas Desulfurization Water in the Coal Combustion System and the Removal of Boron and Mercury from the Water, *Energy Fuels*, 2011, **25**, 3568–3573.

22 M. Owens, P. E. Degremont, H. Goltz, D. Mingee and R. Kelly, in *Proceedings Owens 2011 TraceMR*, 2011.

23 S. Virolainen, T. Wesselborg, A. Kaukinen and T. Sainio, Removal of iron, aluminium, manganese and copper from leach solutions of lithium-ion battery waste using ion exchange, *Hydrometallurgy*, 2021, **202**, 105602.

24 J. T. M. Amphlett, M. D. Ogden, R. I. Foster, N. Syna, K. Soldenhoff and C. A. Sharrad, Polyamine functionalised ion exchange resins: Synthesis, characterisation and uranyl uptake, *Chem. Eng. J.*, 2018, **334**, 1361–1370.

25 J. T. M. Amphlett, S. Choi, S. A. Parry, E. M. Moon, C. A. Sharrad and M. D. Ogden, Insights on uranium uptake mechanisms by ion exchange resins with chelating functionalities: Chelation vs. anion exchange, *Chem. Eng. J.*, 2020, **392**, 123712.

26 Purolite Corporation, Puromet™ MTS9300 – Product Data Sheet, 2021.

27 Purolite Corporation, Puromet™ MTS200 – Product Data Sheet, 2021.

28 K.-L. Chiu and W.-S. Chen, Recovery and separation of valuable metals from cathode materials of spent lithium-ion batteries (LIBs) by ion exchange, *Sci. Adv. Mater.*, 2017, **9**, 2155.

29 Z. Zainol and M. J. Nicol, Comparative study of chelating ion exchange resins for the recovery of nickel and cobalt from laterite leach tailings, *Hydrometallurgy*, 2009, **96**, 283.

30 P. Siqueira, C. D. Silva and I. D. Silva, Nickel and cobalt adsorption in an ion exchange resin as an alternative for treating the leached liquer, *REM, Rev. Esc. Minas*, 2011, **64**, 319.

31 A. Deepatana and M. Valix, Adsorption of Metals from Metal–Organic Complexes Derived from Bioleaching of Nickel Laterite Ores, *ECI Conference on Separations Technology VI: New Perspectives on Very Large-Scale Operations*, 2004.

32 A. M. Bożęcka and S. Sanak-Rydlewska, The use of ion exchangers for removing cobalt and nickel ions from water solutions, *Arch. Min. Sci.*, 2018, **63**(3), 633–646.

33 E. Abdulbur-Alfakhoury and M. Leermakers, Elimination of interferences in the determination of platinum, palladium and rhodium by diffusive gradients in thin films (DGT) and inductively coupled plasma mass spectrometry (ICP MS) using selective elution, *Talanta*, 2021, **223**(2), 121771.

34 P. J. Lloyd-Jones, J. R. Rangel-Mendez and M. Streat, Mercury Sorption from Aqueous Solution by Chelating Ion Exchange Resins, Activated Carbon and a Biosorbent, *Process Saf. Environ. Prot.*, 2004, **82**(4), 301–311.

35 J. P. Gustafsson, *Visual MINTEQ, 3.1*, 2013.

36 D. B. Gingerich and M. S. Mauter, Flue Gas Desulfurization Wastewater Composition and Implications for Regulatory and Treatment Train Design, *Environ. Sci. Technol.*, 2020, **54**(7), 3783–3792.

37 G. Wei, L. Qingcai, W. Chang-Yu, L. Hailong, L. Ying, Y. Jian and W. Guofang, Kinetics of mercury oxidation in the presence of hydrochloric acid and oxygen over a commercial SCR catalyst, *Chem. Eng. J.*, 2013, **220**, 53–60.

38 AEP, *American Electric Power Mercury Removal Effectiveness Report*, 2010.

39 M. Marhol and K. L. Cheng, Some chelating ion-exchange resins containing ketoiminocarboxylic acids as functional groups, *Talanta*, 1974, **21**, 751–762.

40 J. Lehto, A. Paajanen, R. Harjula and H. Leinonen, Hydrolysis and H+/Na+ Exchange by Chelex 100 Chelating Resin, *React. Polym.*, 1994, **23**, 134–140.

41 M. Matzapetakis, B. T. Farrer, T. Weng, L. Hemmingsen, J. E. Penner-Hahn and V. L. Pecoraro, Comparison of the binding of cadmium(II), mercury(II) and arsenic(III) to the de Novo designed peptides TRI L12C and TRI L16C, *J. Am. Chem. Soc.*, 2002, **124**, 8042–8054.